Geophysical Research Letters

RESEARCH LETTER
10.1029/2024GL110331

On the Abnormally Strong Westward Phase of the Mesospheric Semiannual Oscillation at Low Latitudes During March Equinox 2023

Jose Suclupe[1], Jorge L. Chau[1], J. Federico Conte[1], Nicholas M. Pedatella[2], Rolando Garcia[3], Kaoru Sato[4], Christoph Zülicke[1], Lourivaldo M. Lima[5], Guozhu Li[6], S. Vijaya Bhaskara Rao[7], M. Venkat Ratnam[8], Rodolfo Rodriguez[9], and Danny Scipion[10]

[1]Leibniz-Institute of Atmospheric Physics at the University of Rostock, Kühlungsborn, Germany, [2]High Altitude Observatory, NSF National Center for Atmospheric Research, Boulder, CO, USA, [3]Atmospheric Chemistry Observations and Modeling Lab, NSF National Center for Atmospheric Research, Boulder, CO, USA, [4]Department of Earth and Planetary Science, The University of Tokyo, Tokyo, Japan, [5]Universidade Estadual da Paraíba, Campina Grande, Brazil, [6]Beijing National Observatory of Space Environment, Institute of Geology and Geophysics, Chinese Academy of Sciences, Beijing, China, [7]Department of Physics, Sri Venkateswara University, Tirupati, India, [8]National Atmospheric Research Laboratory, Tirupati, India, [9]Universidad de Piura, Piura, Peru, [10]Radio Observatorio de Jicamarca, Instituto Geofísico del Perú, Lima, Peru

Abstract Different meteor radars at low latitudes observed abnormally strong westward mesospheric winds around the March Equinox of 2023, that is, during the first phase of the Mesospheric Semiannual Oscillation. This event was the strongest of at least the last decade (2014–2023). The westward winds reached −80 m/s at 82 km of altitude in late March, and decreased with increasing altitude and latitude. A considerable increase in the diurnal tide amplitude was also observed. The Whole Atmosphere Community Climate Model with thermosphere-ionosphere eXtension constrained to meteorological reanalysis up to ∼50 km does not capture the observed low-latitude behavior. Additionally, these strong mesospheric winds developed during the westerly phase of the Quasi-Biennial Oscillation, in accordance with the filtering mechanism of gravity waves in the stratosphere proposed in previous works. Finally, analysis of SABER temperatures strongly suggests that the breaking of the migrating diurnal tide may be the main driver of these strong winds.

Plain Language Summary Around the March Equinox of 2023, abnormally strong westward winds were observed in the low latitude region at altitudes between 80 and 100 km. This event was the strongest in at least the last decade. The westward winds reached a maximum amplitude of 80 m/s at 82 km of altitude during late March, and decreased with increasing altitude and latitude. A considerable increase in the amplitude of the diurnal tide was also observed. Simulations based on a whole atmosphere global circulation model constrained to meteorological reanalysis up to ∼50 km do not capture the observed behavior. Results based on specular meteor radar and satellite measurements suggest that the strong westward winds were driven by two main factors: the filtering mechanism of eastward-propagating gravity waves in the stratosphere and the breaking of the diurnal tide at about 85 km of altitude.

Key Points:

- Strong mesospheric westward winds during March equinox 2023 are observed globally at low latitudes
- The westward winds reached a peak of −80 m/s at 82 km, the largest in the last ten years, accompanied by an enhancement of the diurnal tide
- The breaking of the DW1 plays a role in generating these strong winds, in addition to the filtering of gravity waves in the stratosphere

Supporting Information:

Supporting Information may be found in the online version of this article.

Correspondence to:

J. Suclupe,
suclupe@iap-kborn.de

Citation:

Suclupe, J., Chau, J. L., Conte, J. F., Pedatella, N. M., Garcia, R., Sato, K., et al. (2024). On the abnormally strong westward phase of the mesospheric semiannual oscillation at low latitudes during March equinox 2023. *Geophysical Research Letters*, *51*, e2024GL110331. https://doi.org/10.1029/2024GL110331

Received 16 MAY 2024
Accepted 23 JUL 2024

Author Contributions:

Conceptualization: Jose Suclupe, Jorge L. Chau, J. Federico Conte, Rolando Garcia, Kaoru Sato, Christoph Zülicke
Formal analysis: Jose Suclupe, Jorge L. Chau, J. Federico Conte, Nicholas M. Pedatella, Rolando Garcia, Kaoru Sato, Christoph Zülicke
Investigation: Jose Suclupe, Jorge L. Chau, J. Federico Conte, Nicholas M. Pedatella, Rolando Garcia, Kaoru Sato, Christoph Zülicke, Lourivaldo M. Lima, Guozhu Li, S. Vijaya Bhaskara Rao, M. Venkat Ratnam, Rodolfo Rodriguez, Danny Scipion
Methodology: Jose Suclupe, Rolando Garcia, Christoph Zülicke

1. Introduction

The Semiannual Oscillation (SAO) in the stratosphere and lower mesosphere was first reported in the 1960s (Reed, 1965, 1966; Reed & Rogers, 1962). In particular, Reed (1966) reported a pronounced SAO between the altitudes of 30 and 65 km using rocketsonde data at Ascension Island (8°S, 14°W). His findings revealed that winds are westward near the solstices and eastward near the equinoxes. Also, Reed (1966) inferred that the maximum amplitude of the SAO occurs at the equator around the stratopause (∼50 km), and that the amplitude subsequently decreases with altitude and latitude. This oscillation is usually referred to as the "stratopause SAO," or SSAO.

Hirota (1978) extended the analysis of the SAO from 30 to 90 km. He reported the existence of a second SAO in the mesopause (MSAO), which is out of phase with respect to the SSAO. The MSAO eastward (westward) peaks appear around the solstices (equinoxes), whereas SSAO eastward (westward) peaks occur around the equinoxes (solstices).

Resources: Jorge L. Chau, Nicholas M. Pedatella, Rolando Garcia, Christoph Zülicke, Lourivaldo M. Lima, Guozhu Li, S. Vijaya Bhaskara Rao, M. Venkat Ratnam, Rodolfo Rodriguez, Danny Scipion
Software: Jose Suclupe, Nicholas M. Pedatella, Rolando Garcia, Christoph Zülicke
Supervision: Jorge L. Chau, J. Federico Conte
Validation: Nicholas M. Pedatella, Rolando Garcia, Kaoru Sato, Christoph Zülicke, Lourivaldo M. Lima, Guozhu Li, S. Vijaya Bhaskara Rao, M. Venkat Ratnam, Rodolfo Rodriguez, Danny Scipion
Visualization: Jose Suclupe, Rolando Garcia
Writing – original draft: Jose Suclupe
Writing – review & editing: Jorge L. Chau, J. Federico Conte, Nicholas M. Pedatella, Rolando Garcia, Kaoru Sato, Christoph Zülicke, Lourivaldo M. Lima, Guozhu Li, S. Vijaya Bhaskara Rao, M. Venkat Ratnam, Rodolfo Rodriguez, Danny Scipion

Garcia et al. (1997) summarized the climatology of the SAO using different instruments such as satellite, ground-based, and rocket measurements. They showed the asymmetry of the MSAO, whose westward phase during the first cycle is considerably stronger than during the second cycle. Furthermore, they observed that the westward phase of the MSAO experiences significant interannual variations. In the context of interannual variability, strong mesospheric westward winds have been reported around the March equinox with radars (e.g., Kishore Kumar et al., 2014) and satellites (Fig 6 in Smith et al. (2017)). At around 82 km, these winds reached −80 m/s, which is significantly more intense than the usual values below −20 m/s in the climatology at low latitudes.

Observations have shown a correlation between the occurrence of the abnormally strong westward winds in the first cycle of the MSAO and the westerly (eastward) phase of the stratospheric Quasi-Biennial Oscillation (QBO) (Burrage et al., 1996; Garcia et al., 1997; Mengel et al., 1995). A possible explanation of this is the filtering in the stratosphere of eastward vertically propagating small-scale gravity waves (Antonita et al., 2008; Dunkerton, 1982) and inertia-gravity waves (intermediate-scale waves) (Sassi & Garcia, 1997; Garcia & Sassi, 1999; R. Lieberman et al., 2006) during the westerly phase of the QBO, allowing the selective upward propagation of westward gravity waves, which could then deposit momentum and contribute to the westward background zonal wind observed in the mesosphere.

Another possible explanation for the strong first cycle of the MSAO is the breaking of the migrating diurnal tide (DW1) due to convective instabilities in the mesosphere and lower thermosphere (MLT) region at and above 85 km (Akmaev et al., 1996; Garcia, 2023; Gurubaran & Rajaram, 2001; R. S. Lieberman & Hays, 1994). Under this mechanism, the DW1 that is undergoing dissipation will impart an acceleration on the zonal-mean zonal wind (e.g., Andrews et al., 1987; R. S. Lieberman, 1997; Lindzen, 1981). Recently, Garcia (2023) confirmed this mechanism by using temperature observations made by the SABER infrared radiometer, and quantified the breaking events, which are more frequent around the equinoxes at low latitudes when the amplitude of DW1 is larger.

It has been observed that the westerly phase of the QBO is a necessary but not sufficient condition for the occurrence of the strong first cycle of the MSAO. In a long-term study, Kishore Kumar et al. (2014) proposed a criterion to explain the exceptions. That is, the occurrence of strong mesospheric westward winds is more likely to happen during the westerly QBO phase, except when there is a strong sudden stratospheric warming (SSW) in the previous (northern hemisphere) winter, which could change the filtering conditions in the stratosphere. Simulations conducted by Zülicke and Becker (2017) supported this criterion. The classification of strong and weak SSWs can be found in Kishore Kumar et al. (2014).

In this work, we investigate the abnormally strong first cycle of the MSAO that occurred around the March equinox of 2023. We study this global event using zonal and meridional winds from five meteor radars at low latitudes (±18°), SABER temperatures, and simulations made with the Specified Dynamics Whole Atmosphere Community Climate Model with thermosphere-ionosphere eXtension (SD-WACCM-X) constrained to an atmospheric reanalysis up to ∼50 km. The paper is structured as follows. In Section 2, we describe the data set and methodology. In Section 3, we present the results. First, we show large-scale dynamics (background winds and solar diurnal tide amplitudes) from 2020 to June 2023 to contextualize the abnormally strong first cycle of the MSAO of March equinox 2023. Second, we show the global morphology of this abnormal cycle using five meteor radars at low latitudes and supplement our results with the SD-WACCM-X simulations. Third, we report zonal meteor winds from 2014 to 2023 between 80 and 100 km to pinpoint the strongest cycles of the last decade. Finally, we present temperature amplitudes of the migrating diurnal tides and other quantities to show the role of tidal breaking in the generation of the strongest cycles between 2014 and 2023. To summarize, in Section 5 we present the concluding remarks.

2. Data Sets and Methodology

2.1. Specular Meteor Radars

We utilized horizontal hourly winds estimated from SIMONe Jicamarca radar located at 11.9°S, 76.8°W from January 2020 to June 2023. This data was used to introduce and highlight the unusual behavior of the westward winds and the diurnal tide around the March equinox in 2023. For more information on the SIMONe Jicamarca radar, please refer to Chau et al. (2021).

To describe the global occurrence of the abnormally strong first cycle of the MSAO in 2023, we have used zonal and meridional winds between 80 and 100 km from January 2022 to June 2023 with resolutions of 1-hr and 2-km (in the vertical). We have considered five meteor radars: (a) SIMONe Jicamarca, at 11.9°S, 76.8°W (Chau et al., 2021; Suclupe et al., 2023); (b) SIMONe Piura, at 5°S, 80°W (Conte et al., 2023; Poblet et al., 2023); (c) Cariri, at 7.4°S, 36.5°W (Buriti et al., 2008); (d) Tirupati, at 13.63°N, 79.4°E (Rao et al., 2014); and (e) Ledong, at 18.4°N, 109°E (Wang et al., 2019).

Additionally, we have used monthly winds from Tirupati from January 2014 to June 2023 to analyze the MSAO around the March equinox during the last ten years.

2.2. WACCM-X

WACCM-X is a whole atmosphere model that extends from the surface to the upper thermosphere (∼500–700 km), and includes the necessary dynamics, chemistry, and physics to simulate the whole atmosphere and ionosphere (Liu et al., 2018). For the present investigation, we have used the Specified Dynamics (SD) configuration, where the model meteorology is constrained by MERRA-2 up to ∼50 km (Smith et al., 2017). This allows for the model state in the troposphere-stratosphere to closely follow the true state of the atmosphere. At higher altitudes the model is unconstrained, and the accuracy of the dynamical variability in the mesosphere is thus partly dependent upon processes internal to the model itself.

We have used two subsets of zonal winds from SD-WACCM-X to study the MSAO. The first data set was used to compare with observations. It covers the period January 2010 to December 2021 and is provided for each of the five radar latitudes (12°S, 7°S, 5°S, 14°N, and 18°N), every 3 hr, 5° in longitude (from 0° to 355°), and ∼2 km altitude resolution at MLT altitudes. The second data set was used to study the reproducibility of the past abnormally strong first cycles of the MSAO, and it covers the interval from 2000 until 2021.

2.3. Mean Winds and Diurnal Tide Estimation

The background (mean) winds, as well as the amplitude and phase of the dominant tides were estimated using a least squares method with a running window of 21 days and 2 km, shifted by 1 day and 1 km, respectively. The fitted periods correspond to 8, 12, 12.42, 24, and 48 hr. The 21-days window was chosen to separate the contributions from the 12-hr and 12.42-hr waves. The last one corresponds to the lunar tide, which could have relatively weak but non-negligible amplitudes (e.g., Sandford and Mitchell (2007)).

2.4. Migrating Diurnal Tide (DW1) From SABER Temperatures

We have estimated the amplitude of the solar migrating diurnal tide (DW1) from temperature observations made by the Sounding of the Atmosphere using Broadband Emission Radiometry (SABER) infrared radiometer (Russell et al., 1994) on NASA's Thermosphere, Ionosphere, Mesosphere Energetics and Dynamics (TIMED) satellite (Yee et al., 2003). Following the methodology of Garcia (2023), the amplitudes were synthesized from the temperature spectrum between frequencies 0.99–1.006 cpd (periods of 0.99–1.01 days). This range of periods includes the diurnal harmonic itself and all the annual, semiannual and quasi-biennial variability of DW1; see Fig. 2 in Garcia (2023) for details. Moreover, we have followed the methodology presented in Section 5 of Garcia (2023) to study the breaking of DW1. After estimating the potential temperature (θ), two parameters were estimated. Those proxies allow us to measure the intensity of the breaking. The first one is the number of breaking events (where the vertical gradient of potential temperature, $d(\theta)/dz$, is negative) per pentad (in a window of 5 days). The second one is the breaking layer depth, which is the average depth of the atmospheric region where $d(\theta)/dz$ is negative.

3. Results

3.1. Planetary-Scale Dynamics Over Jicamarca

In Figure 1, we can see the background winds and the amplitudes of the total diurnal tide in the MLT region over Jicamarca (12°S, 77°W) from January 2020 to June 2023. Additionally, Figure S1 in the Supporting Information S1 shows the amplitudes of the quasi-two-day wave (Q2DW) and the 12-hr and 8-hr tides. It is important to emphasize that a single radar measures total tides, meaning it cannot separate the contribution of migrating (e.g., DW1) and non-migrating tides.

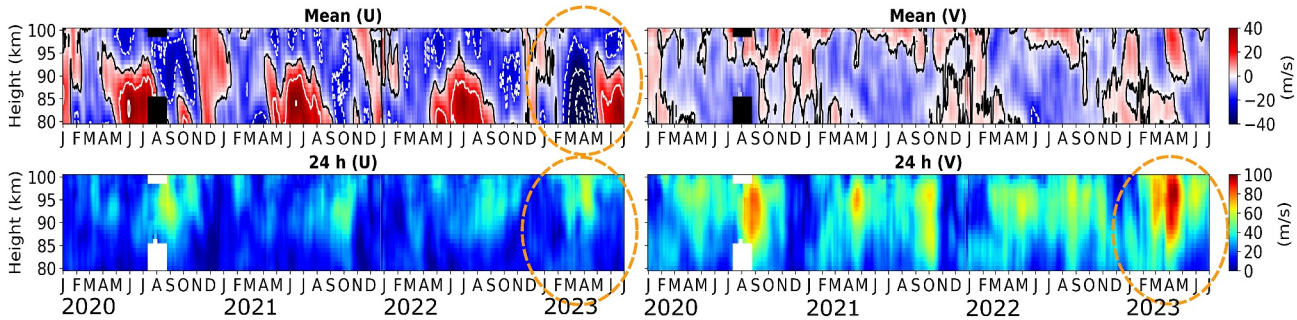

Figure 1. Planetary-scale dynamics in the MLT region obtained by SIMONe Jicamarca, located at 12°S, 77°W. The figure displays the zonal (left column) and meridional (right column) components of the mean wind (first row) and the amplitude of the total 24-hr tide (second row). The orange dashed ovals highlight the unusual winds and tidal amplitudes around March equinox 2023. Data gaps are indicated in black (first row) and white (second row).

These results indicate that from 2020 to 2023, the large-scale dynamics in general follow the climatology previously reported over Jicamarca by Suclupe et al. (2023). That is, the amplitude of the meridional component of the diurnal tide is more intense than that of the zonal one. The 24-hr tide dominates (see Figure S1 in the Supporting Information S1 for the full picture). The meridional diurnal component shows its largest peak in August-September and the second one in April-May, while the zonal diurnal component only shows a clear maximum in August-September. The Q2DW reaches maximum amplitudes in January. The meridional semidiurnal component peaks in April-May (similar to the diurnal tide). The terdiurnal tide generally shows a maximum above 90 km in March-April and September-October (see Figure S1 in the Supporting Information S1). The SAO in the zonal mean wind is observed between 80 and 93 km. The meridional mean winds are mostly southward with weak interannual variability.

The striking feature in these observations is the strong mesospheric westward wind around March equinox 2023, which reveals an abnormally strong first cycle of the MSAO. Also, the diurnal tide presents larger amplitudes around the same period (see the orange dash ovals in Figure 1). In addition, the meridional components of the 12-hr and 8-hr tides also exhibit larger amplitudes around March 2023 over Jicamarca (see Figure S1 in the Supporting Information S1).

3.2. Abnormally Strong First Cycle of the MSAO in March Equinox 2023 at Low Latitudes

Figure 2a shows the zonal background winds from January 2022 to June 2023, measured at five low-latitude radar stations: Jicamarca (12°S, 77°W), Cariri (7°S, 36°W), Piura (5°S, 81°W), Tirupati (14°N, 72°E), and Ledong (18°N, 109°E). Figures 2b and 2c display the zonal background winds for Jicamarca and Ledong at three different altitudes (82, 88, and 94 km) from 2020 to 2023 and 2019 to 2023, respectively. The light-blue shaded region shows the altitudinal average ($\pm 1\sigma$) between 80 and 100 km, of the climatology given by SD-WACCM-X from 2010 to 2021. Figure 2d shows the zonal background winds at 82 km over the five low-latitude stations obtained from 2-a. The light-blue shaded region represents the latitudinal average ($\pm 1\sigma$) between -18 and 18°, of the climatology given by SD-WACCM-X from 2010 to 2021.

Besides the different annual behavior of the zonal winds between the northern and southern hemisphere sites, strong westward winds are observed over all the stations during the March equinox of 2023 (Figure 2a). Even at 30°S over central Chile, an enhancement of the mean zonal wind in the westward direction can be appreciated (not shown here). The strength of these westward winds decreases with altitude (Figures 2b and 2c) and latitude (Figure 2d). The strong westward winds start developing in February, to vanish almost simultaneously at the end of April (same slope, Figure 2d). The westward peak occurs first in the southern stations, from West to East (81°W to 36°W), at the end of March, and then in the northern hemisphere stations, first over Tirupati (72°E) and later over Ledong (109°E) at the beginning of April.

SD-WACCM-X simulations reproduce the MSAO, but with considerably smaller amplitudes. The relatively lower variability of SD-WACCM-X winds observed in Figure 2b–2d, indicates that the model does not capture the abnormally strong first cycle of the MSAO between 2010 and 2021. Furthermore, we investigated the reproducibility of strong westward background winds in the model from 2000 to 2021 at 5°S at 82 km. Then we examined whether strong winds, previously reported in the literature during March-April 2002, 2008, 2011, and

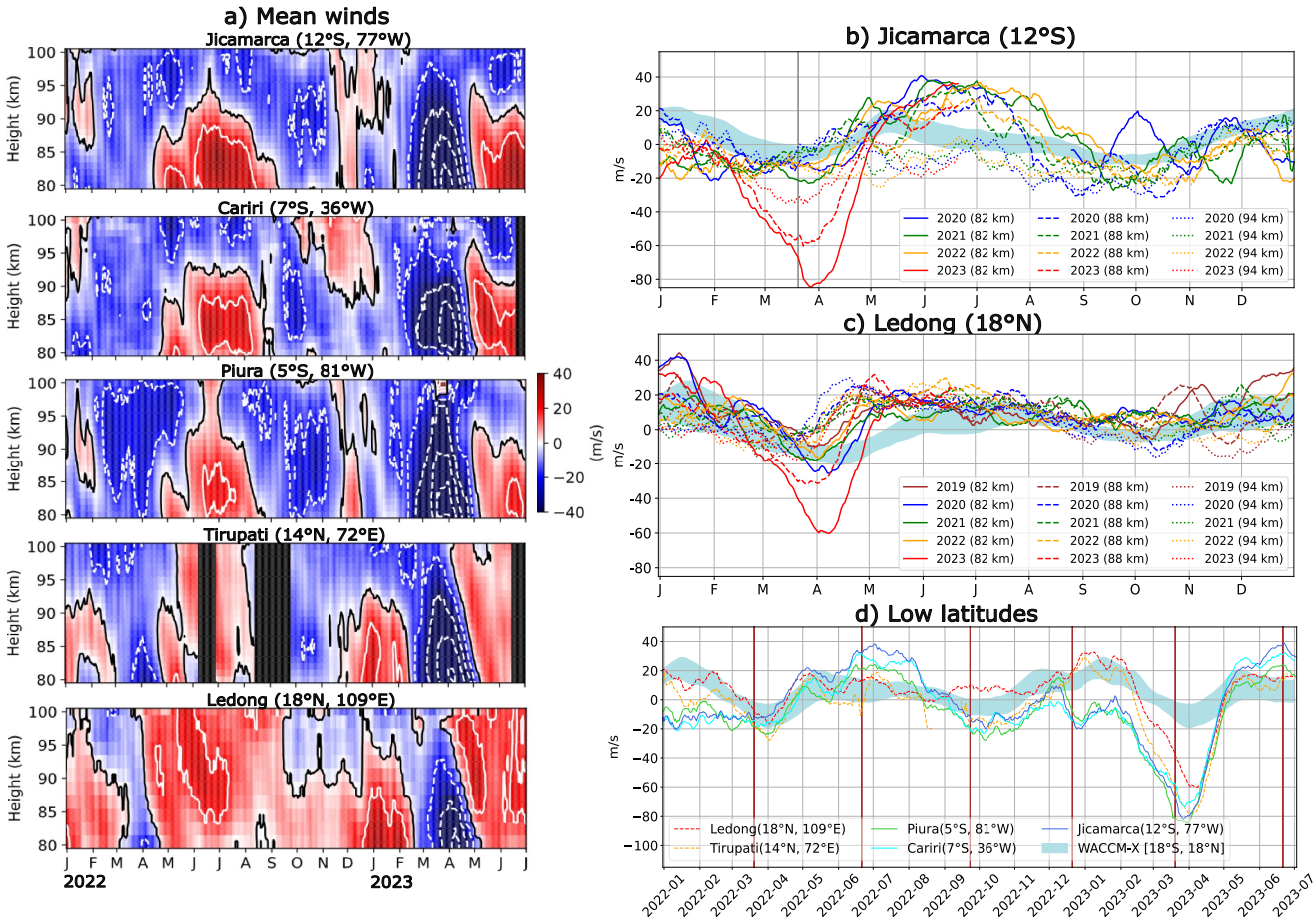

Figure 2. (a) Zonal mean winds from January 2022 to June 2023 obtained by five meteor radars at low latitudes. (b) Yearly zonal mean winds over Jicamarca (12°S) from 2020 to June 2023 at 82, 88, and 94 km. (c) The same as (b) but over Ledong (18°N) from 2019 to June 2023. (d) Zonal mean winds obtained from (a) at 82 km. The light-blue shaded region shows the climatology (average $\pm 1\sigma$) given by SD-WACCM-X from 2010 to 2021. See the text for more details. Data gaps are indicated in black.

2017 (Kishore Kumar et al., 2014), were reproduced by SD-WACCM-X. Figure S2 in the Supporting Information S1 shows that, although the SD-WACCM-X winds in three of the years exceeded 1 σ from the mean of March and April, they never reached 3σ, and they showed smaller amplitudes than in the observations.

3.3. Mesospheric Zonal Winds Over Tirupati

Monthly zonal winds from 2014 to 2023 over Tirupati at 82 km are shown in Figure 3. The light-blue shaded region represents the region of $\pm 1\sigma$ with respect to the mean. The data shows that there was significant variability around the March equinox. The strongest westward winds were observed in 2023, followed by 2017. We applied the classification criterion suggested by Kishore Kumar et al. (2014) to this data set and found that 8 of our 10 cases match their criterion (see the list in Figure 3 for further details). That is, an abnormally strong first cycle of the MSAO, referred to as mesospheric spring equinox enhancement (MSEE) by Kishore Kumar et al. (2014), is favored under the following conditions: when there is a westerly (W) QBO phase, and there was no "Strong" SSW (i.e., "None" or "Weak" class, according to Kumar et al.'s classification). Note that the QBO phase was classified, as in Kishore Kumar et al. (2014), based on the strongest stratospheric westward winds within the region 100–5 hPa (~16–35 km), from the Singapore radiosonde observations, being "Easterly QBO" when it is less than −30 m/s, and "Westerly QBO" in the other cases.

As we can see, the criterion based on the filtering mechanisms of gravity waves in the stratosphere, works from 2014 to 2023, except for 2014 and 2016. Some years are shown in parentheses in Figure 3, since they must be further investigated. For example, in 2014, the QBO was slightly above the threshold; it could have also been easterly. In 2021, the QBO was slightly below the threshold; it could have also been westerly. In 2023, the SSW

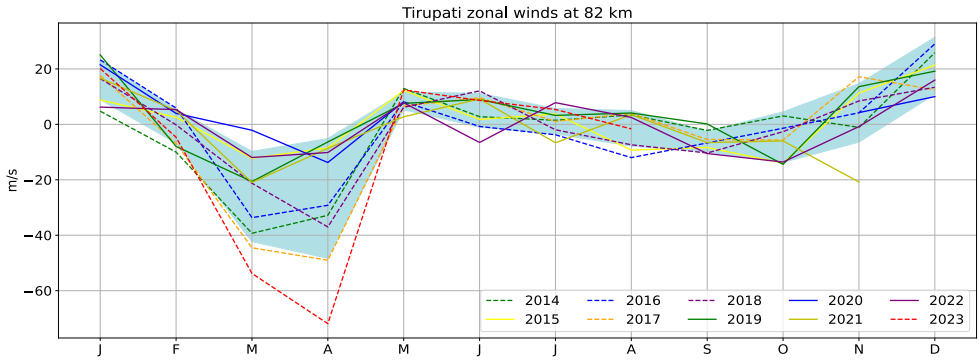

Year	QBO phase	SSW Class	Abnormal first cycle of the MSAO	Criterion Success
2014	**(W)**	**None**	**(Abnormal)**	(Failing)
2015	E	**None**	None	Matching
2016	**W**	**None**	**Abnormal**	Failing
2017	**W**	**None**	**Abnormal**	Matching
2018	E	Strong	None	Matching
2019	**W**	Strong	Missing	Matching
2020	E	**None**	None	Matching
2021	(E)	**Weak**	(None)	(Matching)
2022	E	**None**	None	Matching
2023	**W**	**(Weak)**	**(Abnormal)**	(Matching)

Figure 3. Monthly zonal winds from 2014 to 2023 over Tirupati at 82 km. The light-blue shaded region represents the region of $\pm 1\sigma$ with respect to the mean. The list shows the classification criterion suggested by Kishore Kumar et al. (2014) applied to this data set. Westerly (W) QBO phase, SSW "None" or "Weak," with both resulting in "Abnormal" flag, indicated in bold. The cases indicated in parenthesis must be further investigated.

was formally classified as "Weak," but after some days with weak eastward winds, another westward wind phase began, making the classification unclear.

3.4. DW1 Breaking Observed by SABER

Figure 4 illustrates the behavior of DW1 and its breaking from temperature measurements obtained by SABER. Figure 4a shows the amplitude of DW1 at 12 scale height (about 85 km). As expected, DW1 presents higher amplitudes at low latitudes (±15°). Moreover, the DW1 tide is very large in March equinox 2023. It is also large in 2017, the second year with strong westward zonal winds in March equinox, as indicated by observations over Tirupati (Figure 3).

Figures 4b and 4c show two measures of the tidal breaking over the equator. The first one shows the number of breaking events per pentad; and the second one shows the breaking layer depth, which is indicative of the strength of breaking. The year 2023 stands out on both counts (and so does 2017).

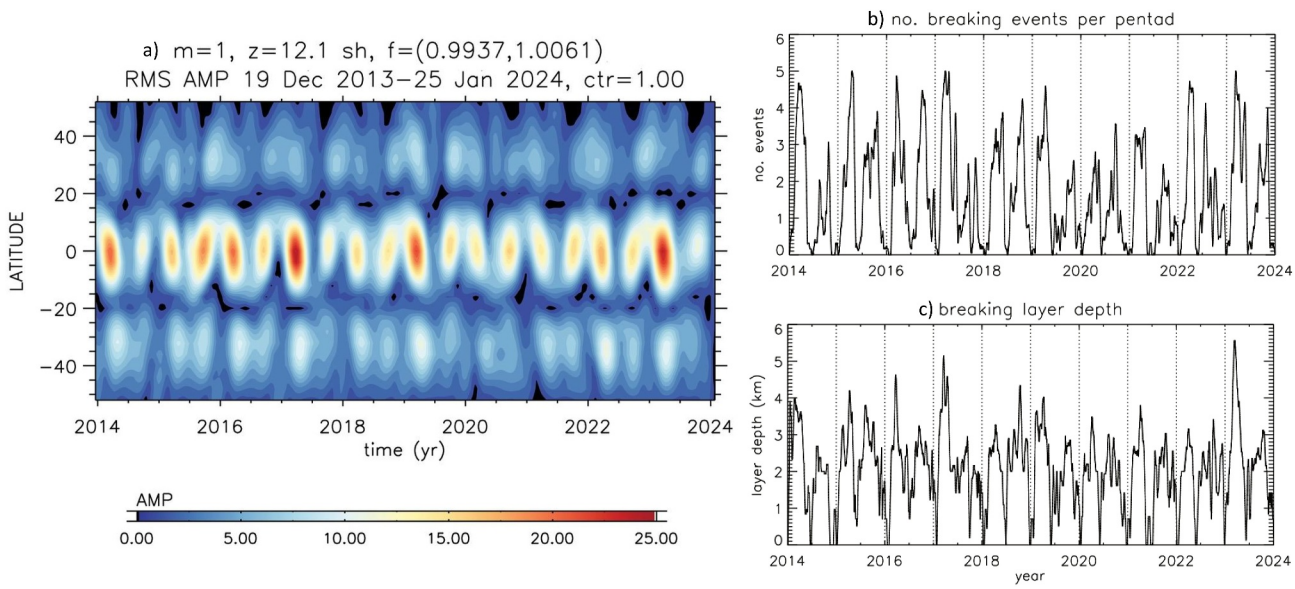

Figure 4. Analysis of DW1 breaking by following the methodology of Garcia (2023). (a) Amplitude of DW1 at 12 sh (about 85 km) obtained from SABER temperatures, (b) number of breaking events per pentad, and (c) the average of the breaking layer depth over the equator.

4. Discussion

Zonal momentum fluxes estimated over SIMONe Jicamarca and SIMONe Piura exhibit a clear enhancement in the westward direction during March 2023 (not shown here), suggesting that mesoscale gravity waves can partially account for the abnormally strong westward winds. Moss et al. (2016) observed over Ascension Island (8°S, 14°W) that strong westward fluxes of high-frequency gravity waves are not always sufficient to produce abnormally strong westward winds during the March equinox. They suggested that other forcing should be involved in order to fully explain the appearance of those strong westward winds.

Garcia (2023) showed that the migrating diurnal tide breaks due to convective instabilities at and above ∼85 km around the equinoxes, but more frequently around the March equinox. Analysis of SABER temperatures revealed a peak in DW1 amplitude at ∼84 km in March 2023 (results not shown here) with a breaking layer depth of around 5 km. Furthermore, our analysis indicates that there were outstanding and strong DW1 breaking events around the March equinox 2023. This supports the breaking of DW1 as another driver of the abnormally strong westward mesospheric winds.

It has been expected that the meridional advection of angular momentum from higher latitudes enhances the equatorial westward flow related to the SSAO near the stratopause (∼50 km) in the solstitial seasons (Smith et al., 2023; Tomikawa et al., 2008). The meridional advection is carried out by the deep branch of the Brewer-Dobson circulation in the stratosphere and can cause large interannual variability, because the speed of the deep branch reflects the Eliassen-Palm (EP) flux divergence due to planetary waves, which mainly determines the presence or absence of sudden stratospheric warmings at winter high latitudes. However, it is unclear how important the meridional advection of angular momentum is in the upper mesosphere, where the strong westward winds are observed. This issue is left for future studies.

The comparison of SD-WACCM-X simulations with previously reported abnormally strong westward winds (in March 2002, 2008, 2011, and 2017) shows that the model reproduces winds that exceed the mean by over one standard deviation, but with much weaker amplitudes than the events reported in the observations. This could be because the MSAO is generally too weak in WACCM (Gettelman et al., 2019; Richter & Garcia, 2006), which is likely related to poor representation of the gravity wave activity. Since SD-WACCM-X shares the same physics/dynamics in the mesosphere with WACCM, it would have the same issue. Inadequate representation of the wave forcing may also account for the weaker westward winds during the strong cycles of the MSAO.

The strongest westward winds, which reached values larger than −80 m/s, were reported at low latitudes (Day & Mitchell, 2013; Garcia et al., 1997; Kishore Kumar et al., 2014) in 1993 and 2002. In our study, we report a new case in 2023. The occurrence of these strongest westward winds in March 2023 satisfies the conditions of the filtering mechanisms in the stratosphere proposed by Kishore Kumar et al. (2014): they developed during the Westerly phase of the QBO, and there was no Strong SSW class in the previous northern hemisphere winter.

Lossow et al. (2008) reported the climatology between 2002 and 2006 of mesospheric water vapor measurements taken by the Sub-Millimetre Radiometer (SMR) instrument aboard the Odin satellite. They showed an asymmetric variability around 75 km over low latitudes during the equinoxes, with a higher peak around the March equinox. Considering that strong westward winds were also reported in March 2002, this suggests that the events with abnormally strong westward phases of the mesospheric semiannual oscillation could affect water vapor transport around this altitude. Moreover, it is expected that the strong westward flow itself modulates the filtering of the upward propagation of gravity waves and affects the circulation in the region of the lower thermosphere and above so that this process could modulate the transport of minor constituents at this region.

5. Concluding Remarks

In this study, we have reported the strongest westward winds during the first phase of the mesospheric SAO in the last ten years (2014–2023). They developed around the March equinox of 2023, at low latitudes. Meteor radar observations show that the westward winds reached −80 m/s (more than three standard deviations with respect to a three-year climatology) at 82 km of altitude, and decreased with altitude and latitude. On the other hand, the abnormally strong westward winds are not reproduced in SD-WACCM-X simulations.

Temperature measurements made by SABER suggest that the breaking of the diurnal tide plays a significant role in accelerating the zonal mean winds. Besides, these abnormally strong westward winds took place during the

westerly phase of the QBO, which supports the filtering mechanism of eastward-propagating gravity waves in the stratosphere. Thus, the here reported abnormally strong westward winds must be the result of momentum deposition by both westward-propagating gravity waves and the DW1 tide.

Data Availability Statement

The data used to produce the radar results is available in NETCDF4 format in Suclupe (2024). All the winds from SD-WACCM-X model used in this work can be found in Gasperini (2019). SABER data can be found in https://data.gats-inc.com/saber/.

Acknowledgments
This work is part of an internal project at the Leibniz-Institute of Atmospheric Physics called LoLa. The Ledong meteor radar is part of the MIOS, supported by the National Natural Science Foundation of China (42020104002 and 41727803). The S. J. do Cariri meteor radar is operated by Observatório de Luminescência Atmosférica da Paraíba (OLAP) UFCG from collaboration with INPE. This material is based upon work supported by the National Center for Atmospheric Research, which is a major facility sponsored by the U.S. National Science Foundation under Cooperative Agreement 1852977. This research was partially supported by the International Space Science Institute (ISSI) in Bern and Beijing, through ISSI/ISSI-BJ International Team project "The mesosphere and lower thermosphere at low latitudes (MLT-LoLa): its day-to-day variability and its contributions to thermospheric/ionospheric weather" (ISSI Team project #23-571; ISSI-BJ Team project #59). KS was supported by JSPS KAKENHI Grant JP22H00169. We would like to acknowledge high-performance computing support from Derecho (Computational and Information Systems Laboratory, 2023) provided by NSF-NCAR's Computational and Information Systems Laboratory, sponsored by the National Science Foundation. NP acknowledges support from NASA Grants 80NSSC20K1350 and 80NSSC20K0721. Open Access funding enabled and organized by Projekt DEAL.

References

Akmaev, R. A., Forbes, J. M., & Hagan, M. E. (1996). Simulation of tides with a spectral mesosphere/lower thermosphere model. *Geophysical Research Letters*, *23*(16), 2173–2176. https://doi.org/10.1029/96gl01977

Andrews, D. G., Holton, J. R., & Leovy, C. B. (1987). *Middle atmosphere dynamics (No. 40)*. Academic press.

Antonita, T. M., Ramkumar, G., Kumar, K. K., & Deepa, V. (2008). Meteor wind radar observations of gravity wave momentum fluxes and their forcing toward the mesospheric semiannual oscillation. *Journal of Geophysical Research*, *113*(D10), D10115. https://doi.org/10.1029/2007jd009089

Buriti, R. A., Hocking, W. K., Batista, P. P., Medeiros, A. F., & Clemesha, B. R. (2008). Observations of equatorial mesospheric winds over Cariri (7.4°S) by a meteor radar and comparison with existing models. *Annales Geophysicae*, *26*(3), 485–497. https://doi.org/10.5194/angeo-26-485-2008

Burrage, M., Vincent, R., Mayr, H., Skinner, W., Arnold, N., & Hays, P. (1996). Long-term variability in the equatorial middle atmosphere zonal wind. *Journal of Geophysical Research*, *101*(D8), 12847–12854. https://doi.org/10.1029/96jd00575

Chau, J. L., Urco, J. M., Vierinen, J., Harding, B. J., Clahsen, M., Pfeffer, N., et al. (2021). Multistatic specular meteor radar network in Peru: System description and initial results. *Earth and Space Science*, *8*(1), e01293. https://doi.org/10.1029/2020EA001293

Computational and Information Systems Laboratory. (2023). Derecho: HPE Cray EX System (NCAR Community Computing). NSF National Center for Atmospheric Research. https://doi.org/10.5065/qx9a-pg09

Conte, J. F., Chau, J. L., Yiğit, E., Suclupe, J., & Rodríguez, R. (2023). Investigation of mesosphere and lower thermosphere dynamics over central and northern Peru using SIMONe systems. *Journal of the Atmospheric Sciences*, *81*(1), 93–104. https://doi.org/10.1175/jas-d-23-0030.1

Day, K., & Mitchell, N. (2013). Mean winds in the MLT, the SQBO and MSAO over ascension island (8 S, 14 W). *Atmospheric Chemistry and Physics*, *13*(18), 9515–9523. https://doi.org/10.5194/acp-13-9515-2013

Dunkerton, T. J. (1982). Theory of the mesopause semiannual oscillation. *Journal of the Atmospheric Sciences*, *39*(12), 2681–2690. https://doi.org/10.1175/1520-0469(1982)039<2681:totmso>2.0.co;2

Garcia, R. R. (2023). On the structure and variability of the migrating diurnal temperature tide observed by SABER. *Journal of the Atmospheric Sciences*, *80*(3), 687–704. https://doi.org/10.1175/JAS-D-22-0167.1

Garcia, R. R., Dunkerton, T. J., Lieberman, R. S., & Vincent, R. A. (1997). Climatology of the semiannual oscillation of the tropical middle atmosphere. *Journal of Geophysical Research*, *102*(22), 19–26. https://doi.org/10.1029/97jd00207

Garcia, R. R., & Sassi, F. (1999). Modulation of the mesospheric semiannual oscillation by the quasibiennial oscillation. *Earth Planets and Space*, *51*(7–8), 563–569. https://doi.org/10.1186/bf03353215

Gasperini, F. (2019). 1980-2017 specified dynamics (SD) WACCM-X version v2.1 simulation with nudging of MERRA-2 data [Dataset]. *UCAR/NCAR Climate Data Gateway*. https://doi.org/10.26024/5B58-NC53

Gettelman, A., Mills, M., Kinnison, D., Garcia, R., Smith, A., Marsh, D., et al. (2019). The whole atmosphere community climate model version 6 (WACCM6). *Journal of Geophysical Research: Atmospheres*, *124*(23), 12380–12403. https://doi.org/10.1029/2019jd030943

Gurubaran, S., & Rajaram, R. (2001). Mean winds, tides, and gravity waves during the westward phase of the mesopause semiannual oscillation (MSAO). *Journal of Geophysical Research*, *106*(D23), 31817–31824. https://doi.org/10.1029/2001jd000325

Hirota, I. (1978). Equatorial waves in the upper stratosphere and mesosphere in relation to the semiannual oscillation of the zonal wind. *Journal of the Atmospheric Sciences*, *35*(4), 714–722. https://doi.org/10.1175/1520-0469(1978)035<0714:ewitus>2.0.co;2

Kishore Kumar, G., Kishore Kumar, K., Singer, W., Zülicke, C., Gurubaran, S., Baumgarten, G., et al. (2014). Mesosphere and lower thermosphere zonal wind variations over low latitudes: Relation to local stratospheric zonal winds and global circulation anomalies. *Journal of Geophysical Research*, *119*(10), 5913–5927. https://doi.org/10.1002/2014JD021610

Lieberman, R., Riggin, D., Garcia, R., Wu, Q., & Remsberg, E. (2006). Observations of intermediate-scale diurnal waves in the equatorial mesosphere and lower thermosphere. *Journal of Geophysical Research*, *111*(A10), A10S11. https://doi.org/10.1029/2005ja011498

Lieberman, R. S. (1997). Long-term variations of zonal mean winds and (1, 1) driving in the equatorial lower thermosphere. *Journal of Atmospheric and Solar-Terrestrial Physics*, *59*(13), 1483–1490. https://doi.org/10.1016/s1364-6826(96)00150-2

Lieberman, R. S., & Hays, P. B. (1994). An estimate of the momentum deposition in the lower thermosphere by the observed diurnal tide. *Journal of the Atmospheric Sciences*, *51*(20), 3094–3105. https://doi.org/10.1175/1520-0469(1994)051⟨3094:AEOTMD⟩2.0.CO;2

Lindzen, R. S. (1981). Turbulence and stress owing to gravity wave and tidal breakdown. *Journal of Geophysical Research*, *86*(C10), 9707–9714. https://doi.org/10.1029/jc086ic10p09707

Liu, H.-L., Bardeen, C. G., Foster, B. T., Lauritzen, P., Liu, J., Lu, G., et al. (2018). Development and validation of the whole atmosphere community climate model with thermosphere and ionosphere extension (WACCM-x 2.0). *Journal of Advances in Modeling Earth Systems*, *10*(2), 381–402. https://doi.org/10.1002/2017ms001232

Lossow, S., Urban, J., Gumbel, J., Eriksson, P., & Murtagh, D. (2008). Observations of the mesospheric semi-annual oscillation (MSAO) in water vapour by Odin/SMR. *Atmospheric Chemistry and Physics*, *8*(21), 6527–6540. https://doi.org/10.5194/acp-8-6527-2008

Mengel, J. G., Mayr, H. G., Chan, K. L., Hines, C. O., Reddy, C. A., Arnold, N. F., & Porter, H. S. (1995). Equatorial oscillations in the middle atmosphere generated by small scale gravity waves. *Geophysical Research Letters*, *22*(22), 3027–3030. https://doi.org/10.1029/95gl03059

Moss, A. C., Wright, C. J., Davis, R. N., & Mitchell, N. J. (2016). Gravity-wave momentum fluxes in the mesosphere over Ascension Island (8°S, 14°W) and the anomalous zonal winds of the semi-annual oscillation in 2002. *Annales Geophysicae*, *34*(2), 323–330. https://doi.org/10.5194/angeo-34-323-2016

Poblet, F. L., Chau, J. L., Conte, J. F., Vierinen, J., Suclupe, J., Liu, A. Z., & Rodriguez, R. R. (2023). Extreme horizontal wind perturbations in the mesosphere and lower thermosphere over South America associated with the 2022 Hunga Eruption. *Geophysical Research Letters*, *50*(12), e2023GL103809. https://doi.org/10.1029/2023GL103809

Rao, S. V. B., Eswaraiah, S., Venkat Ratnam, M., Kosalendra, E., Kishore Kumar, K., Sathish Kumar, S., et al. (2014). Advanced meteor radar installed at Tirupati: System details and comparison with different radars. *Journal of Geophysical Research*, *119*(21), 11893–11904. https://doi.org/10.1002/2014JD021781

Reed, R. J. (1965). The quasi-biennial oscillation of the atmosphere between 30 and 50 km over ascension island. *Journal of the Atmospheric Sciences*, *22*(3), 331–333. https://doi.org/10.1175/1520-0469(1965)022<0331:tqboot>2.0.co;2

Reed, R. J. (1966). Zonal wind behavior in the equatorial stratosphere and lower mesosphere. *Journal of Geophysical Research*, *71*(18), 4223–4233. https://doi.org/10.1029/jz071i018p04223

Reed, R. J., & Rogers, D. G. (1962). The circulation of the tropical stratosphere in the years 1954–1960. *Journal of the Atmospheric Sciences*, *19*(2), 127–135. https://doi.org/10.1175/1520-0469(1962)019<0127:tcotts>2.0.co;2

Richter, J. H., & Garcia, R. R. (2006). On the forcing of the mesospheric semi-annual oscillation in the whole atmosphere community climate model. *Geophysical Research Letters*, *33*(1), 2–5. https://doi.org/10.1029/2005GL024378

Russell, J. M., Mlynczak, M. G., & Gordley, L. L. (1994). Overview of the sounding of the atmosphere using broadband emission radiometry (SABER) experiment for the thermosphere-ionosphere-mesosphere energetics and dynamics (TIMED) mission. *Optical Spectroscopic Techniques and Instrumentation for Atmospheric and Space Research*, *2266*, 406–415.

Sandford, D., & Mitchell, N. (2007). Lunar tides in the mesosphere over ascension island (8°S, 14.4°W). *Annales Geophysicae*, *25*(1), 9–12. https://doi.org/10.5194/angeo-25-9-2007

Sassi, F., & Garcia, R. R. (1997). The role of equatorial waves forced by convection in the tropical semiannual oscillation. *Journal of the Atmospheric Sciences*, *54*(15), 1925–1942. https://doi.org/10.1175/1520-0469(1997)054<1925:troewf>2.0.co;2

Smith, A. K., Garcia, R. R., Moss, A. C., & Mitchell, N. J. (2017). The semiannual oscillation of the tropical zonal wind in the middle atmosphere derived from satellite geopotential height retrievals. *Journal of the Atmospheric Sciences*, *74*(8), 2413–2425. https://doi.org/10.1175/JAS-D-17-0067.1

Smith, A. K., Lesley, J. G. J., & García, R. R. (2023). Evidence for the influence of the quasi-biennial oscillation on the semiannualoscillation in the tropical middle atmosphere. *Journal of the Atmospheric Sciences*, *80*(7), 1755–1769. https://doi.org/10.1175/JAS-D-22-0255.1

Suclupe, J. (2024). On the abnormally strong westward phase of the mesospheric semiannual oscillation at low latitudes during March equinox 2023 [Dataset]. *RADAR — Research Data Repository*. https://doi.org/10.22000/GjDVNfgQbxfgOsuq

Suclupe, J., Chau, J. L., Conte, J. F., Milla, M., Pedatella, N. M., & Kuyeng, K. (2023). Climatology of mesosphere and lower thermosphere diurnal tides over Jicamarca (12°S, 77°W): Observations and simulations. *Earth Planets and Space*, *75*(1), 186. https://doi.org/10.1186/s40623-023-01935-z

Tomikawa, Y., Sato, K., Watanabe, S., Kawatani, Y., Miyazaki, K., & Takahashi, M. (2008). Wintertime temperature maximum at the subtropical stratopause in a T213l256 GCM. *Journal of Geophysical Research*, *113*(D17), D17117. https://doi.org/10.1029/2008jd009786

Wang, Y., Li, G., Ning, B., Yang, S., Sun, W., & Yu, Y. (2019). All-sky interferometric meteor radar observations of zonal structure and drifts of low-latitude ionospheric E region irregularities. *Earth and Space Science*, *6*(12), 2653–2662. https://doi.org/10.1029/2019EA000884

Yee, J.-H., Rodberg, E., Harvey, R. J., Kusnierkiewicz, D. Y., Knopf, W., Grunberger, P., et al. (2003). Advanced technology and mission operations concepts employed on NASA'S timed mission. *Space systems Technology and Operations*, *5088*, 43–52.

Zülicke, C., & Becker, E. (2017). Relation between equatorial mesospheric wind anomalies during spring and middle atmosphere variability modes. *Scientific Online Letters on the Atmosphere*, *13A*(Specialedition), 31–35. https://doi.org/10.2151/sola.13A-006